Structure of dormant bacterial ribosomes reveals an elusive translation factor with evolutionary connections to eukaryotic protein synthesis factors

Authors

Karla Helena-Bueno[1], Chinenye L. Ekemezie[1], Charlotte R. Brown[1], Arnaud Baslé[1], James N. Blaza[2], Chris H. Hill[3], Sergey V. Melnikov[1]

Affiliations

[1] Biosciences Institute, Newcastle University, Newcastle upon Tyne, UK
[2] Department of Chemistry and York Biomedical Research Institute, University of York, York, UK
[3] Department of Biology and York Biomedical Research Institute, University of York, York, UK

To whom correspondence should be addressed

chris.hill@york.ac.uk
sergey.melnikov@newcastle.ac.uk

During starvation and stress, virtually all organisms arrest their protein synthesis and convert their ribosomes into a state of dormancy in which a special class of proteins, known as hibernation factors, protect the ribosome from damage. In bacteria, two major families of hibernation factors have been characterized, but the low conservation of these proteins and the huge diversity of species, habitats and environmental stressors has made the discovery of new dormancy factors challenging. In this study, we identify a new bacterial protein involved in ribosome dormancy. We first characterize dormant ribosomes following cold shock in the psychrophilic bacterium *Psychrobacter urativorans* using proteomics and cryo-EM. We show that during cold shock, ribosomes in this organism associate with a previously uncharacterized protein that occupies ribosomal active centres and multiple drug-binding sites. Our structure reveals that this new factor, which we term Balon, bears no resemblance to known bacterial hibernation factors. Instead, it belongs to a family of bacterial homologs of the eukaryotic translation factor aeRF1. We identify unique motifs present only in Balon but not its archaeal or eukaryotic counterparts that allow it to engage with the peptidyl transferase center and decoding center of dormant bacterial ribosomes. We then show that, across the bacterial kingdom, Balon-encoding genes are found in nearly 20% of known species and are located in operons involved in different types of stress responses, including osmotic and thermal shock, hypoxia, acid, tRNA damage and antibiotic stress. Taken together, our work shows that bacterial cells possess a functional homolog of eukaryotic translation termination factor, which is likely repurposed into a stress-response protein. This finding illuminates a long-sought evolutionary connection between the bacterial and eukaryotic protein synthesis machinery.

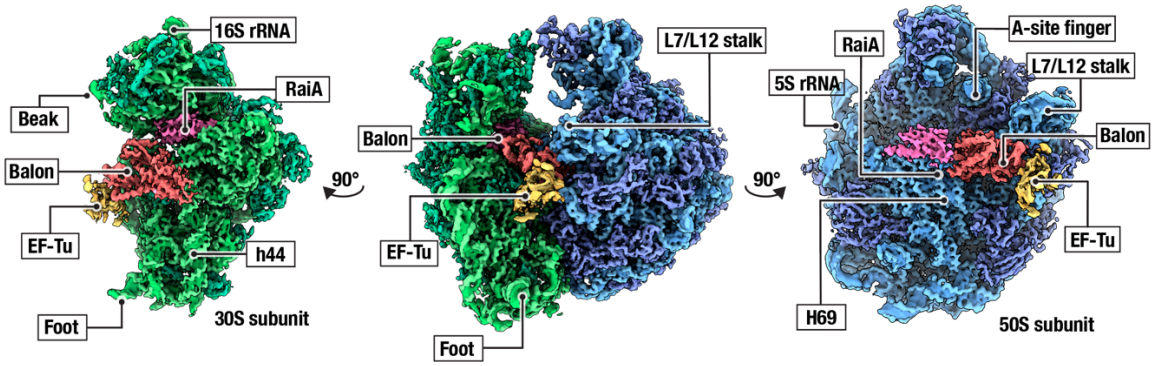

Fig 1 | Cryo-EM analysis of dormant ribosomes from cold-adapted bacteria *P. urativorans* reveals Balon, a new factor in bacterial protein synthesis. (**A**) Cryo-EM structure (3.65 Å) of ribosomes from bacteria *P. urativorans*, isolated during cold shock. The density map is colour-coded and shown in three orthogonal views. Nearly half of ribosomes in the sample are not engaged in protein synthesis, evident by the absence of mRNA or tRNA molecules and presence of the hibernation factor RaiA. These non-translating ribosomes associate with a newly identified protein Balon that appears to be delivered to the ribosomal A site by the elongation factor EF-Tu. (**B**-**D**) Cryo-EM map (mesh) and refined atomic models (sticks) showing molecular details of Balon-ribosome interactions. Direct contacts between Balon and 30S, EF-Tu and 50S are observed.

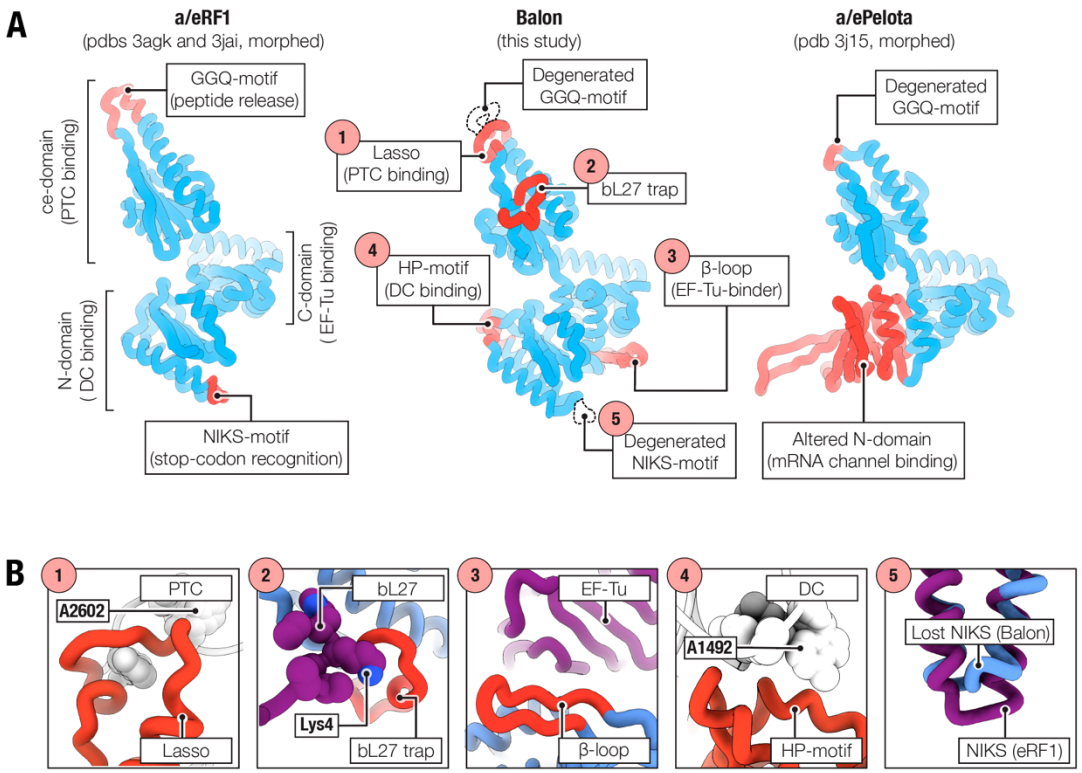

Fig 2 | Balon resembles proteins aeRF1 and Pelota, suggesting a shared evolutionary history with the aeRF1-family of archaeo-eukaryotic translation factors. (**A**) Comparison illustrating structural similarity between Balon, aeRF1 and Pelota proteins. Balon more closely resembles the translation termination factor aeRF1: it shares a common domain organization and binds the ribosome in a similar way via contacts with EF-Tu, the decoding centre (DC) and the peptidyl-transferase centre (PTC). Balon lacks structural features that are required for aeRF1 activity, including the NIKS-motif (stop-codon recognition) and the GGQ-motif (nascent peptide release). These features are also absent in Pelota, another archaeo-eukaryotic ribosome rescue factor. (**B**) Five unique structural features (labelled) distinguish Balon from both aeRF1 and Pelota and allow Balon to bind dormant bacterial ribosomes.

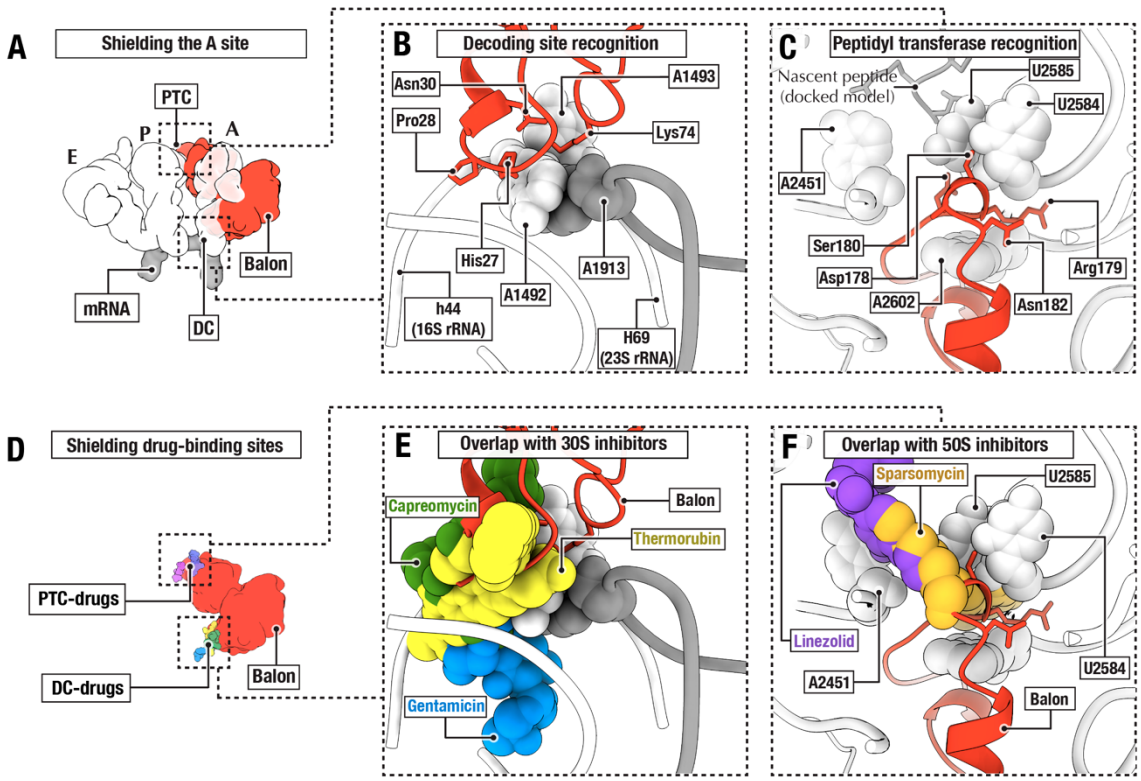

Fig 3 | Balon occupies ribosomal active centres and overlaps with multiple drug-binding sites. (**A**) Superposition of Balon (red), tRNAs (white) and mRNA (grey) to compare ribosomal binding sites of these molecules. Balon occupies the ribosomal A site—the primary entry site of protein synthesis substrates. (**B**) Zoomed-in view of the decoding centre of the ribosome, showing details of small subunit recognition by Balon. Similar to aeRF1 and Pelota, Balon binds the ribosomal decoding centre. However, unlike aeRF1 and Pelota, Balon uses a unique HP-motif (red) which allows binding to the decoding centre without making contacts with mRNA or the mRNA entry channel. This mRNA-independent recognition strategy allows Balon to bind ribosomes concurrently with the hibernation factor RaiA. (**C**) Zoomed-in view of the peptidyl-transferase centre of the ribosome, showing details of large subunit recognition by Balon. Like aeRF1 and Pelota, Balon binds the vicinity of the peptidyl-transferase centre of the ribosome. However, unlike aeRF1 and Pelota, Balon contacts the peptidyl-transferase residue U2585 using a lasso-like protein loop (red) that wraps around the drug-binding residue A2602. (**D**) Superposition of Balon (red) and eight ribosome-targeting antibiotics (colour coded) shows that Balon occludes binding sites for drugs targeting both the peptidyl-transferase centre (PTC-drugs) and the decoding centre (DC-drugs). (**E, F**) Zoomed-in views of the decoding centre and the peptidyl-transferase centre. Balon binds multiple ribosomal drug-binding residues, overlapping with the binding sites of several families of ribosome-targeting antibiotics.

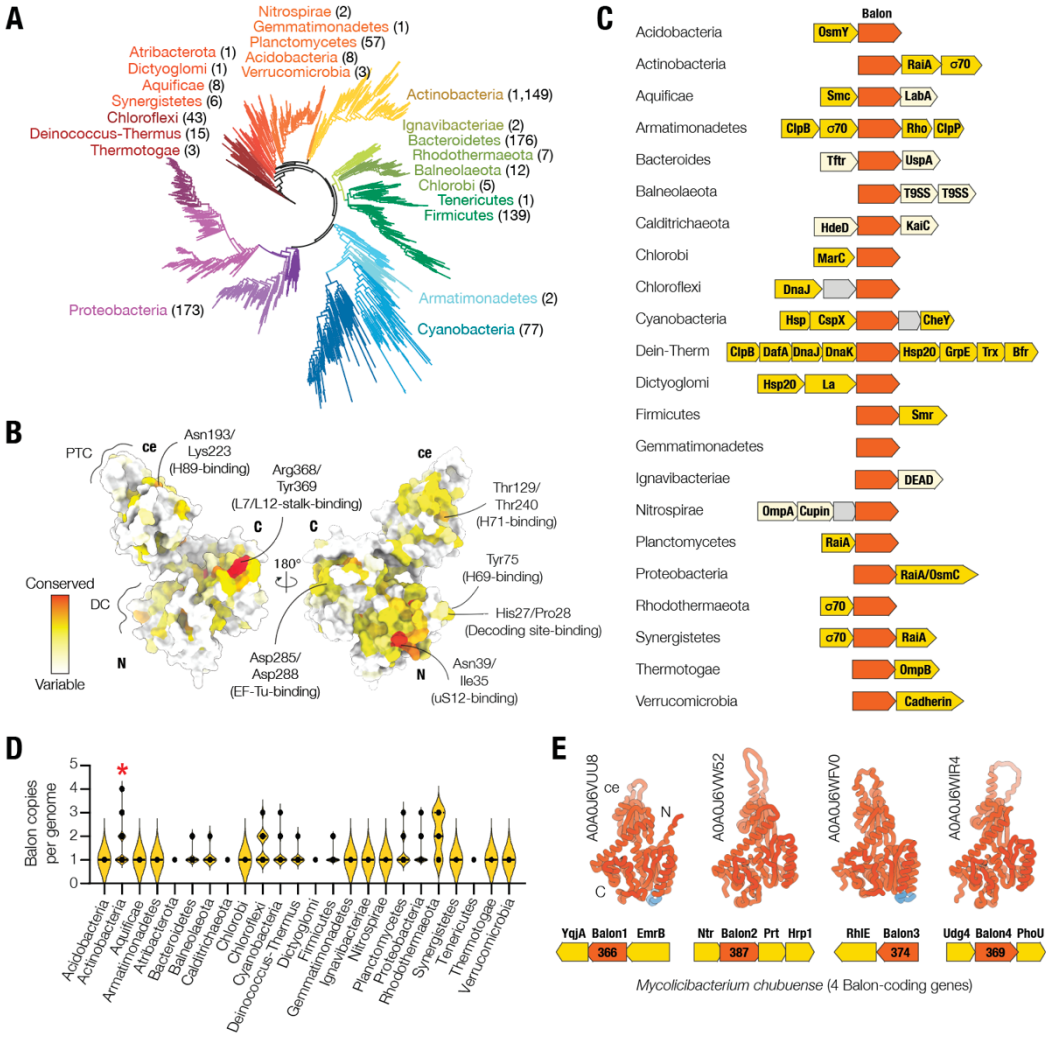

Fig 4 | Balon-coding genes are widespread among bacteria and are often found in stress-response operons. (**A**) The bacterial tree of life shows that Balon homologs are found in most bacterial lineages including 23 different phyla with 1,572 representative bacteria containing detectable Balon homologs. (**B**) Atomic model of Balon (coloured by sequence conservation) illustrates high conservation of residues responsible for ribosome recognition. (**C**) Schematic operon structures show a few examples of genetic surroundings of Balon-coding genes in various bacterial phyla. Although Balon-coding genes have a highly variable genomic surrounding between phyla, Balon-coding genes are typically found in operons that encode stress response factors. These include heat- and cold-shock response proteins (such as chaperones Hsp20, DnaK, DnaJ), alternative σ70 factors, factors of acid tolerance (HdeD) and osmotic stress tolerance (OsmB and OsmY), ribosome hibernation (RaiA), ribosome and tRNA repair (RtcB), and multidrug resistance (Smr, MarC, EmrB). (**D**) In 38% of the bacterial species analyzed (603 species), Balon homologs are encoded by two, three or four gene copies located in different genomic loci, suggesting their independent expression. (**E**) An example of *Mycolicibacterium chubuense* shows four copies of Balon-coding genes, with one copy (Balon 1) residing in an operon with the multidrug export protein EmrB, and another copy (Balon 2) located in an operon with hypoxia-response factors. The structures (predicted by Alphafold), although similar, possess variations relative to each other. Overall, Balon is a widely occurring bacterial protein with homologs found in ~20% of representative bacterial species.

INTRODUCTION

Protein synthesis, also known as translation, is a critical step of gene expression that is catalysed by the ribosome—a megadalton supercomplex, comprising 3-4 rRNA molecules and over 50 ribosomal proteins[1]. Ribosome assembly represents an enormous metabolic investment, occupying up to ~70 % of transcriptional bandwidth[2-4]. Therefore, when cells experience starvation or environmental stress, protein synthesis is often reversibly paused, and ribosomes enter a state of 'suspended animation' until conditions improve[5-8]. This preservation of existing ribosomes in a functionally intact state is essential for cell survival.

Although the reversible arrest of protein synthesis was initially viewed as a passive process in which ribosomes remain idle and free from ligands, it has become clear in recent years that, during starvation and stress, ribosomes associate with a specialized group of cellular proteins known as hibernation factors or dormancy factors[9,10]. These factors bind to ribosomes, shielding their vulnerable active centres from degradation by cellular nucleases[11-13]. Due to this critical protective role, the depletion of dormancy factors causes the accumulation of damaged ribosomes and drastically impairs the ability of cells to recover their growth after starvation, stress, or drug treatment[14-17].

Ribosome dormancy factors have been found in some species, yet it is unknown how many exist in nature. To date, several families of ribosome-dormancy factors have been characterized in eukaryotes, including protein Stm1 in yeast[18], Serpbp1 and Irfd2 in mammals[19,20], Lso2 in mammals and fungi[21-23], and Mdf1 in the fungal parasites microsporidia[24,25]. Also, two major families of dormancy factors were found in bacteria, including the RaiA family (including RaiA, Hpf and LrtA), found in many bacterial lineages, and Rmf, found in some γ-proteobacteria[9,26-28]. Overall, these studies revealed that, unlike most other translation factors, ribosome dormancy factors are highly diverse and lack conservation even within a single domain of life, thus making finding new hibernation factors challenging.

Structural analyses of dormant ribosomes from several species revealed that factors involved in ribosome dormancy comprise an array of structurally dissimilar proteins that bind different sites in the ribosome[18-26]. Nonetheless, all dormancy factors share one property: their ability to protect the most critically important functional sites in the ribosome, such as the mRNA channel and tRNA-binding sites[9]. Furthermore, some dormancy factors have non-overlapping binding sites, making it possible for the ribosome to simultaneously bind several dormancy factors[11-13,26]. However, the lack of universal conservation of ribosome dormancy factors, along with a small number of suitable organisms to study ribosome dormancy, leaves it unclear to what extent findings made in common model organisms—mainly *E. coli* —can be considered generally representative.

In this study, by introducing a new model organism for ribosome dormancy studies, the bacterium *Psychrobacter urativorans*, we identify a previously unknown factor which appears to be involved in ribosome dormancy, which we name Balon due to its structural similarity to the archaeo-eukaryotic protein synthesis factor Pelota (Spanish for "Ball"). Our cryo-EM analysis reveals the unique capacity of Balon to bind to the ribosomal A site, where Balon shields two active centres of the ribosome and overlaps with binding sites of multiple families of ribosome-targeting antibiotics. Our structure suggests that Balon is a distant and structurally diverged homolog of the eukaryotic translation factor eRF1. This finding corroborates previous bioinformatic annotations in which hypothetical genes of eRF1-like proteins were found in numerous bacterial species[29-31]. Our structure highlights key differences between Balon and aeRF1, explaining how Balon engages with dormant ribosomes instead of translating ribosomes. Finally, using a sensitive homology search, we identify Balon-coding genes in nearly 20 % of studied bacteria, illustrating their prevalence throughout the bacterial kingdom. Overall, our work identifies a previously unknown bacterial ribosome dormancy factor, describing a previously unknown mode by which bacteria preserve their ribosomes during stress. On a broader level, we provide experimental evidence of functional eukaryotic-like translation factors in bacteria, illuminating a long-sought evolutionary connection between bacterial and eukaryotic protein synthesis machinery.

Results

Cryo-EM analysis of ribosomes from the cold-adapted bacterium *P. urativorans* identifies a new factor of bacterial protein synthesis, Balon

Our interest in ribosome hibernation arose from our studies of the molecular adaptations of protein synthesis to cold temperatures, using the bacterium *P. urativorans* as a model organism. *P. urativorans* is a notorious cold-adapted organism that often spoils frozen food due to its ability to grow at sub-zero temperatures[32-35]. In the laboratory, *P. urativorans* has the recommended growth temperature of 10°C, but in nature *P. urativorans* can survive colder environments, including Antarctic permafrost soil and glacial ice[32].

To understand how *P. urativorans* adapts its translation apparatus to sudden decreases in temperature, we studied their ribosomes under cold shock conditions. Because *P. urativorans* are slowly growing bacteria, with a doubling time greater than one week, we first grew cultures for multiple weeks at 10°C to produce sufficient biomass. We then exposed these growing cultures to ice for 30 minutes and isolated their ribosomes for proteomic and cryo-EM analyses (**Materials and Methods**). Previously, sudden decreases in temperature in organisms like *E. coli* and *B. subtilus* were shown to cause a rapid and nearly complete arrest and protein synthesis within the first few minutes, followed by a gradual recovery in the following hours[36-38]. We, therefore, anticipated a transient arrest in protein synthesis in *P. urativorans* in response to the ice treatment. Consistently, we found that after exposure to ice, approximately half of *P. urativorans* ribosomes disengage from protein synthesis, as evidenced by the absence of aminoacyl-tRNAs and mRNAs in the decoding centre and their association with the hibernation factor RaiA, indicating their dormant status (**Figs. 1 and S1**). Strikingly, these dormant ribosomes were also associated with the elongation factor EF-Tu and a previously uncharacterized protein, which we name Balon (**Fig. 1, Figs. S1-S3**). Thus, our cryo-EM analysis revealed a new apparent factor of protein synthesis associated with dormant ribosomes from the ice-treated *P. urativorans* cells.

Balon resembles archaeal and eukaryotic factors of protein synthesis

To reveal the identity and better understand the evolutionary origin and molecular function of Balon, we assessed whether Balon belongs to any studied protein family. Using our cryo-EM map, we first built a poly-alanine model of Balon, and then used this model to search for structurally similar proteins across the Protein Data Bank (**Fig. 2**, **Table S2, Methods**). Our search revealed greatest structural similarity to proteins from archaea and eukaryotes, with Balon most closely resembling aeRF1-family members. This family includes two known ribosome-binding proteins: the protein aeRF1, a translation termination factor that binds the ribosomal A site and terminates protein synthesis in response to mRNA stop codons, and the protein Pelota, a ribosome-rescue factor that binds the A site on ribosomes that are arrested by aberrant mRNAs[17,39,40]. Our subsequent mass-spectrometry analysis of our crude ribosome samples revealed the identity and sequence of Balon—a 41kDa protein, which is currently annotated as a hypothetical protein AOC03_06830 (**Supplementary Data 1**).

Our structure-guided sequence alignment showed that Balon shares just ~10 % sequence identity with both aeRF1 and Pelota, yet these three proteins have a similar overall architecture (rmsd < 4.0 Å for their structurally conserved Cα atoms). Furthermore, these three proteins have a similar length of ~370 (Balon), ~400 (aRF1) and ~410 amino acids (Pelota) and the same domain organization, including the N-terminal domain that binds the small ribosomal subunit, the central domain that binds the large ribosomal subunit, and the C-terminal domain that binds protein EF-Tu. (**Fig. 2, Fig. S3-S5**). This structural similarity can explain the simultaneous presence of EF-Tu and Balon in our ribosome samples: in archaea, EF-Tu delivers both aeRF1 and Pelota to the ribosomal A site to stimulate translation termination or ribosome rescue, respectively[41]. Our cryo-EM analysis shows that Balon has the same ability to bind EF-Tu, suggesting a conserved mechanism of aeRF1, Pelota and Balon delivery to the ribosome by EF-Tu (**Fig. 1**, **Fig. S3**). Also, this structural similarity indicates a common evolutionary origin for Balon, aeRF1 and Pelota and shows that bacteria possess a functional translation factor from the aeRF1-family. Importantly, this represents the first experimental evidence of functional eukaryotic-like translation factors in bacteria.

Balon occupies ribosomal active centres and multiple drug-binding sites

To understand the mechanism by which Balon recognizes idle ribosomes during the cold-shock response, we analyzed its interactions with the ribosome from our cryo-EM structure. Balon spans two active centres of the ribosome: the decoding centre and the peptidyl-transferase centre (**Fig. 3A-C**). Notably, the binding site for Balon overlaps with multiple binding sites of ribosome-targeting antibiotics, including such as tuberactinomycins[42], oxazolidinones[43], as well as thermorubin[44] and sparsomycin[45] (**Fig. 3D-F**).

To recognize the decoding centre, Balon uses a unique strategy compared to aeRF1 and Pelota (**Fig. 3B**). Unlike aeRF1, Balon lacks the characteristic NIKS-motif necessary for mRNA stop codon recognition[46,47]. Unlike Pelota, Balon lacks

the characteristic β-loop that allows Pelota to bind the vacant mRNA channel[48-50]. Instead, Balon has a distinctive HP-motif that directly binds the decoding centre residues A1492 in helix h44, and A1913 in helix H69 (using the *E. coli* rRNA numbering) (**Fig. 3B**). These direct contacts with the decoding centre allow Balon to stay ~10Å away from the mRNA-binding site. This mRNA-independent recognition allows Balon to bind ribosomes simultaneously with the hibernation factor RaiA, which would be impossible for aeRF1 or Pelota due to a steric clash between their N-terminal domains and RaiA (**Fig. S5**).

To recognize the peptidyl-transferase centre, Balon uses an idiosyncratic mechanism to recognize 23S rRNA. Unlike aeRF1, Balon lacks the characteristic GGQ-motif that allows aeRF1 to trigger the nascent peptide release[51]. Instead, Balon bears a lasso-like protein loop that wraps around an rRNA nucleotide (A2602 in the 23S rRNA), positioning Balon adjacent to the outer wall of the peptidyl-transferase centre. In this position, Balon remains excluded from the catalytic centre by U2585 (**Fig. 3C**). There, Balon contacts another component of the bacterial peptidyl transferase centre—ribosomal protein bL27, the N-terminus of which is known to stimulate the activity of the peptidyl-transferase centre[52,53]. Balon moves the N-terminus of bL27 away from the peptidyl-transferase centre using its "bL27-trap", a 20 amino acid-long protein loop in the central domain that distinguishes Balon from both aeRF1 and Pelota. This bL27 binding appears to help Balon access the peptidyl-transferase centre in bacterial ribosomes. Thus, the overall similarity to aeRF1 and Pelota allows Balon to bind the ribosomal A site, but distinctive structural features—such as the HP-motif, the lasso-loop and the bL27-trap—appear to help Balon to bind idle bacterial ribosomes.

Balon is a widespread bacterial protein that is often encoded by stress-response operons

We next sought to understand how conserved Balon might be across bacteria, and we performed a Markov model-based homology search, using the database of reference proteomes. Our search revealed Balon homologs in 1,573 out of 8,761 representative bacteria from 23 of 27 major bacterial phyla. In all these species, Balon homologs have a similar length, lack the GGQ and NIKS/NIKL motifs, but possess characteristic N-terminal insertions that are required for Balon association with the decoding site of the ribosome (**Fig. 4A, B, Supplementary Data 2-6**).

Our homology search also revealed that Balon-coding genes typically reside in stress-response operons: while some these genes were previously annotated as aeRF1-like genes in the vicinity of RaiA genes[30,31], we observed this genetic colocalization mainly in Proteobacteria, Actinobacteria and Planctomycetes. In other phyla, however, Balon-coding genes are located in operons that encode versatile stress response factors, including response factors to thermal shock (e.g. Hsp20), osmotic stress (e.g. OsmC, OsmY), acid (e.g. HdeD), tRNA damage (RtcB) or antibiotics (e.g. MarC, EmrB) (**Fig. 4C, Fig. S8**). Intriguingly, we also observed that many bacteria (603 representative species) possess multiple copies of Balon-coding genes, ranging from 2 to 4 copies per genome (**Fig. 4D**). For example, human pathogens species *Mycobacterium* bear up to four copies of Balon-coding genes, with one of these genes located in the vicinity of the hypoxia-response factor Hrp1, and another being adjacent to the gene encoding the multidrug transporter EmpB (**Fig. 4E**).

Because our cryo-EM structure has captured ribosome binding to both Balon and RaiA, we finally assessed how many of the Balon-bearing bacteria also encode RaiA (**Fig. S9, Supplementary Data S7, S8**). Our analysis of reference proteomes showed that RaiA-type proteins are found in nearly all representative bacteria (~98% of bacteria in the reference proteome database), and Balon is found 18% of RaiA-bearing species. In contrast, we found that Balon-bearing species almost never encode Rmf. Our homology search in reference proteomes identified Rmf in about 5% of representative bacteria, but only 0.2% of the representative bacteria—such as pathogenic species of *Pseudomonas*, *Vibrio* and *Yersinia*—simultaneously bear Rmf and Balon, as well as RaiA (**Fig. S9**).

Discussion

Balon as the first experimental evidence of the existence of elusive eukaryote-type factors of protein synthesis in bacterial cells

It has been a long-standing hypothesis that eukaryote-type translation factors may exist in bacteria, which would indicate an archaeo-eukaryotic evolutionary origin for some components of bacterial translation[29-31,54]. Previous comparative analyses of bacterial genomes revealed hypothetical homologs of eukaryotic and archaeal factors of protein synthesis in many bacterial species. These apparent homologs were initially identified for translation initiation factors, including eIF2, eIF3, eIF4A and eIF6[54]. More recently, various bacteria were shown to have up to 15 families of putative homologs of the archaeo-eukaryotic translation factor aeRF1[30,31]. Consequently, many lineages of bacteria were estimated to have nearly twice as many translation factors compared to the conventional estimates based on the current understanding of bacterial protein synthesis.

However, these computational analyses were inconclusive: sequences of hypothetical homologs of archaeo-eukaryotic translation factors were found to be highly variable or fragmented in bacteria, in contrast to their high conservation in eukaryotes and archaea; and these genes were found only in a fraction of bacterial species, in contrast to their omnipresence in archaea and eukaryotes[54,55]. This sporadic occurrence and high sequence variability—along with the lack of experimental studies of these putative proteins—raised a question: are these proteins functional in bacterial cells? And if so, do they act as bacterial translation factors?

Our finding that Balon belongs to the aeRF1-family of translation factors provides answers to these questions and illustrates how bacteria can evolve some of their dormancy factors. The structural resemblance between Balon and aeRF1 proteins suggests that Balon-coding genes could have originated either directly from aeRF1-coding genes or from their common ancestor through gradual degeneration of the GGQ- and NIKS-motifs that inactivated the undesired ability of this protein to catalyse the nascent peptide release or bind mRNA codons, whereas the subsequent evolution of the HP-motif allowed Balon to evolve the ability to bind hibernating ribosomes in cooperation with the hibernation factor RaiA. Regardless of this evolutionary scenario, our finding of Balon as a functional aeRF1-type protein in bacteria provides the first proof that bacteria encode a functional archaeo-eukaryote-type factor of protein synthesis. This finding reveals that bacteria and eukaryotes share a higher similarity in their machinery of protein synthesis than suggested by conventional models of protein synthesis, although high evolutionary divergence of their shared aeRF1 factors allows the bacterial kingdom to use these factors as a stress response mechanism in contrast to their requirement for basal translation in eukaryotic cells.

Balon as a factor involved in ribosomal dormancy

Here, by investigating an understudied psychrophilic bacterium under the conditions of cold stress, we have identified a new family of bacterial proteins associated with dormant ribosomes. Adding to the two previously known protein families involved in bacterial ribosome dormancy, the family that Balon belongs to is markedly different: sharing structural and sequence similarity with archaeal and eukaryotic translation factors, rather than bacterial ones. Our data reveals how this factor recognizes idle bacterial ribosomes, providing the first structural blueprints of a previously unknown mechanism by which bacteria can preserve their ribosomes during stress.

Our evolutionary analysis demonstrates that Balon-like genes are highly prevalent in bacteria, occurring in nearly 20% of studied bacterial species. Intriguingly, some of these genes have been previously characterized in *Mycobacterium* species, where Balon homologs have been annotated as "uncharacterized protein Rv2629"[56]. In *Mycobacterium tuberculosis*, *Rv2629* gene was identified as a member of the dosR cellular dormancy regulon that is transcriptionally inactive during the log-phase but activated when *M. tuberculosis* enter a cellular dormancy state [56]. Furthermore, *Rv2629* gene expression was shown to be induced by hypoxia, leading to enhanced rifampicin resistance and increased survival and pathogenicity of *Mycobacterium* in mice[57,58]. Also, in *Mycobacterium tuberculosis*, Balon-coding gene is located in the same operon as RtcB, a tRNA splicing factor that repairs stalled and colliding ribosomes and damaged tRNA molecules during starvation and stress[59-62]. Collectively, these previous findings are consistent with our designation of Balon as a ribosome dormancy factor and suggest that bacteria can upregulate Balon expression in response to stress.

The next important step will be to understand how bacterial cells could benefit from having Balon. Because both Rmf and RaiA protect ribosomes from nucleolytic degradation during starvation and stress[11-13], it is possible that Balon functions in an analogous manner, protecting the ribosomal A site that remains vulnerable even in the presence of Rmf and RaiA (**Fig. S9**). It will be also important to understand the mechanism by which Balon is conditionally recruited to ribosomes. Because our study reveals Balon interactions with EF-Tu, it is possible that Balon recruitment could be stimulated by an accumulation of free EF-Tu under stress conditions, when cells reduce availability of major EF-Tu partners, aminoacyl-tRNAs[63].

MATERIALS AND METHODS

Production of *P. urativorans* biomass. As a model organism, we used the bacterium *Psychrobacter urativorans.* (The word *Psychrobacter* originates from "psychro" meaning "cold" and "bacter" meaning "rod", and "urativorans" originates from "uratum" meaning "salt of uric acid" and "vorans" meaning "devouring", which collectively stands for a cold-adapted rod-shape bacterium / uric acid). Freeze-dried cells of *P. urativorans* were obtained from the American Type Culture Collection (ATCC 15174). The cell pellet was rehydrated in 15 mL of pre-chilled Marine Broth 2216 media (Sigma-Aldrich) and incubated in a shaker (SciQuip Incu-Shake Mini) at 150 rpm at 10°C for 7 days, according to the ATCC protocol. This culture was then used to inoculate 1L of pre-chilled Marine Broth 2216 media and incubated at 150 rpm for 4 days at 10 °C until the culture reached an OD_{600} of 0.272. The cells were then transferred on ice for 10 min and centrifuged for 5 min at 4°C and 5,000 g, yielding approximately 1 g of cell pellet.

Ribosome isolation. To lyse the cells, the pellet was rapidly resuspended in 1 mL of buffer A (50mM Tris-HCl pH 7.5, 20 mM $Mg(OAc)_2$, and 50 mM KCl), transferred to 2 mL microcentrifuge tubes containing approximately 0.1 mL of 0.5 mm zirconium beads (Sigma-Aldrich BeadBug™), and disrupted by shaking for 30 sec at 6.5 m/s speed in a bead beater (Thermo FastPrep FP120 Cell Disrupter). The sample was then centrifuged for 5 min at 4°C and 16,000 g to remove cell debris, and the resulting supernatant was collected and centrifuged for 1 min at 16,000 rpm and 4°C to remove the remaining debris. The lysate was then mixed with PEG 20,000 (25% w/v) to a final concentration of 0.5% (w/v) and centrifuged for 5 min at 4°C and 16,000 g to precipitate insoluble aggregates. Then, the supernatant was mixed with PEG 20,000 (powder) to the final concentration of ~19% (w/v) and centrifuged for 5 min at 4°C and 16,000 g to precipitate ribosomes. The obtained pellet was dissolved in 50 µL of buffer A, and the solution was passed twice through PD Spin Trap G-25 microspin columns (GE Healthcare) to clear crude ribosomes from small molecules. The obtained solution had an OD_{260} of 34.89 and $OD_{260/280}$ of 1.71, corresponding to a ribosome concentration of 512 nM. This solution was split into 10 µL aliquots and frozen at -80 °C for subsequent cryo-EM and mass spectrometry analyses.

Mass-spectrometry analysis of crude samples of *P. urativorans* ribosomes. A 10 µL aliquot of crude *P. urativorans* ribosomes solution was reduced with 4.5 mM dithiothreitol and heated at 55°C. The sample was alkylated with the addition of 10 mM iodoacetamide before proteolytic digestion with 0.2 µg Promega sequencing grade trypsin and incubation at 37°C for 16 h. The resulting peptides were desalted by Millipore C18 ZipTip, following the manufacturer's protocol, with final elution into aqueous 50% (v/v) acetonitrile. Desalted peptides were dried under vacuum before being resuspended in aqueous 0.1% trifluoroacetic acid (v/v) for LC-MS/MS.

Peptides were loaded onto a mClass nanoflow UPLC system (Waters) equipped with a nanoEaze M/Z Symmetry 100 Å C18, 5 µm trap column (180 µm x 20 mm, Waters) and a PepMap, 2 µm, 100 Å, C18 EasyNano nanocapillary column (75 µm x 500 mm, Thermo). The trap wash solvent was aqueous 0.05% (v/v) trifluoroacetic acid and the trapping flow rate was 15 µL/min. The trap was washed for 5 min before switching flow to the capillary column. Separation used gradient elution of two solvents: solvent A, aqueous 0.1% (v/v) formic acid; solvent B, acetonitrile containing 0.1% (v/v) formic acid. The flow rate for the capillary column was 330 nL/min and the column temperature was 40°C. The linear multi-step gradient profile was: 3-10% B over 7 mins, 10-35% B over 30 mins, 35-99% B over 5 mins and then proceeded to wash with 99% solvent B for 4 min. The column was returned to initial conditions and re-equilibrated for 15 min before subsequent injections.

The nanoLC system was interfaced with an Orbitrap Fusion Tribrid mass spectrometer (Thermo) with an EasyNano ionization source (Thermo). Positive ESI-MS and MS2 spectra were acquired using Xcalibur software (version 4.0, Thermo). Instrument source settings were: ion spray voltage—1,900 V; sweep gas—0 Arb; ion transfer tube temperature—275°C. MS1 spectra were acquired in the Orbitrap with 120,000 resolution, the scan range of m/z 375-1,500; the AGC target of 4e5, and the max fill time of 100 ms. Data dependent acquisition was performed in top speed mode using a 1 s cycle, selecting the most intense precursors with charge states >1. Easy-IC was used for internal calibration. Dynamic exclusion was performed for 50 s post precursor selection and a minimum threshold for fragmentation was set at 5e3. MS2 spectra were acquired in the linear ion trap with: scan rate—turbo; quadrupole isolation—1.6 m/z; activation type—HCD; activation energy—32%; AGC target—5e3; first mass—110 m/z; max fill time—100 ms. Acquisitions were arranged by Xcalibur to inject ions for all available parallelizable time.

Peak lists in Thermo .raw format were converted to .mgf using MSConvert (version 3.0, ProteoWizard) before submitting to database searching against the *P. urativorans* subset of the UniProt database (3rd Aug 2022, 2,349 sequences; 769,448 residues)[64] appended with 118 common proteomic contaminants. Mascot Daemon (version 2.6.0, Matrix Science) was used to submit the search to a locally-running copy of the Mascot program (Matrix Science Ltd., version 2.7.0). Search criteria specified: enzyme—trypsin; max missed cleavages—2; fixed modifications—carbamidomethylation of protein C-termini; variable modifications—acetylation of protein N-termini, deamidation of Asn and Gln residues, N-terminal conversion of Gln and Glu to pyro-Glu, oxidation of Met, and phosphorylation of Ser, Thr and Tyr residues; peptide tolerance—3 ppm; MS/MS tolerance—0.5 Da; instrument—ESI-TRAP. Peptide identifications were passed through the percolator algorithm to achieve a 1% false discovery rate assessed against a

reverse database. The search data are summarized in (**Supplementary Data 1**), where molar percentages of each identified protein were calculated from Mascot emPAI values by expressing individual values as a percentage of the sum of all emPAI values in the sample, according to Ref.[65].

Cryo-EM grid preparation and data collection. To prepare ribosome samples for cryo-EM analyses, 10 µL aliquots of crude ribosomes were thawed on ice and loaded onto glow discharged (20mA, 90s, PELCO easiGlow) Quantifoil grids (R1.2/1.3, 200 mesh, copper), using 2 µL of the sample per grid. The grids were then blotted for 1 or 2 sec at 100% humidity (using blotting force -5) and vitrified using liquid nitrogen-cooled ethane in a Vitrobot Mark IV (Thermo Fisher Scientific). The grids were then used for data collection with a 200 kV Glacios electron cryo-microscope (Thermo Scientific) with Falcon 4 detector located at the Department of Chemistry of the University of York, UK. For each movie, the grids were exposed to a total dose of 50 e/Å2 across 7 seconds. A nominal magnification of 150,000 was applied, resulting in a final calibrated object sampling of 0.934 Å pixel size. 3,706 micrograph movies were recorded in aberration free image shift (AFIS) mode using a defocus targets of -1.25, -1.0, -0.75, -0.5 µm.

Cryo-EM data processing. Cryo-EM data for the *P. urativorans* dataset were initially processed using cryoSPARC v3.3.2[66] as shown in (**Fig. S1, Fig. S2**). In brief, after patch motion correction and CTF estimation, a total of 811,859 particles were picked from the 3,706 micrographs using cryoSPARC blob picker (Minimum particle diameter 180Å, Maximum particle diameter 220Å). Particles were then extracted using a box size of 700 pixels and subjected to 2 rounds of 2D classification. The resulting classes (62,815 particles) were selected for ab-initio reconstruction and heterogenous refinement with C1 symmetry, which resulted in the map with a resolution of 3.23 Å. This map was used to build a model of the *P. urativorans* ribosome and ribosome-associated proteins. At this point, some heterogeneity was observed at the Balon binding site and decoding centre. To resolve this, the dataset was repicked and reprocessed with RELION 3.1[67] for focused classification (**Fig. S1, Fig. S2**). Particles were extracted in a 450 pixel box and subjected to several rounds of 2D classification prior to initial 3D refinement using the cryoSPARC map as an initial reference, low-pass filtered to 80 Å. Following this, polishing, CTF refinement and post-processing produced a map of 3.2 Å resolution. Angular assignments from this refinement job were used to carry out a masked classification without alignment, focusing on the Balon density and decoding centre. The final subset of Balon-occupied particles (10,632) was refined and post-processed (3.65 Å). Finally, a local resolution map was calculated (3.1 – 9.7 Å). All reported estimates of resolution are based on the gold standard Fourier shell correlation (FSC) at 0.143, and the calculated FSC is derived from comparisons between reconstructions from two independently refined half-sets.

Model building, refinement and deposition. The atomic models of *P. urativorans* ribosomes and the ribosome-binding proteins were produced using Coot v0.8.9.2[68] and AlphaFold[69]. As a starting model, we used the atomic model of ribosomal proteins generated by AlphaFold and the atomic model of rRNA from the coordinates of *Thermus thermophilus* ribosomes (PDB id 4y4o)[70]. These rRNA and protein models were morph-fitted into the cryoSPARC cryo-EM map using ChimeraX[71] and Phenix[72] and then rebuilt using Coot based on the information about the genomic sequence of *P. urativorans* (RefSeq GCF_001298525.1).

The density corresponding to Balon was initially identified as a non-ribosomal protein, which was initially modeled as a poly-alanine chain to determine its backbone structure. This poly-alanine backbone model was then used as an input file for a search of proteins with similar fold in the Protein Data Bank using the NCBI tool for tracking structural similarities of macromolecules, Vast[73]. This search identified the archaeal protein aeRF1 from *Aeropyrum pernix* as the most similar known structure to Balon, suggesting that Balon is a bacterial homolog of aeRF1 (**Table S2**). We therefore searched for *P. urativorans* proteins that have a similar sequence to that of *A. pernix* aeRF1. Using three iterations of Markov model-based search with HHMER[74] in the UniProtKB database, we found that *P. urativorans* encodes a hypothetical protein (Uniport id A0A0M3V8U3) with sequence similarity to aeRF1 and Pelota. This protein, which we termed Balon, had a sequence that matched the cryo-EM map and was used to create its atomic model. The resulting atomic structure of Balon in complex with the ribosome, RaiA and EF-Tu were then refined using Phenix real space refinement, and the refined coordinates were validated using MolProbity[75] and deposited in the Protein Data Bank with the accession number XXXX*.

Evolutionary analysis of Balon. To assess phylogenetic distribution of Balon in bacterial species, we performed three iterations of homology search using the sequence of Balon from *P. urativorans* (Uniprot id A0A0M3V8U3) as an input for a profile hidden Markov Model-based analysis with HMMER[74]. For each search iteration, we used the following search options: -E 1 --domE 1 --incE 0.01 --incdomE 0.03 --seqdb uniprotrefprot. The resulting dataset was reduced first by removing protein sequences that lacked information about their Phylum (21 sequences), then by removing sequences that were shorter than 300 amino acids as they typically lacked one or two of the three domains of Balon/aeRF1 (which included 806 sequences), then by removing sequences that were annotated as a protein fragment (34 sequences), and finally by removing duplicated sequences (31 sequences). This resulted in the dataset including 1,896 sequences of Balon homologs from 1,565 bacterial species (**Supplementary Data 2**).

To gain insight into a possible evolutionary origin of Balon from the archaeo-eukaryotic family of aeRF1 proteins, we performed a complementary analysis in which we sought for bacterial homologs of the archaeal aRF1 using three iterations of HMMER[74]. As an input for the first iteration, we used the sequence of aRF1 from the archaeon *A. pernix*

(pdb id Q9YAF1), which structure was identified in this study among the closest structural homologs of Balon. For each iteration, we used the database of Reference Proteomes restricted to the bacterial domain of life, using these search options: -E 1 --domE 1 --incE 0.01 --incdomE 0.03 --seqdb uniprotrefprot. The resulting dataset was reduced first by removing sequences lacking information about their Phylum (21 sequences), then by removing sequences which were lacking at least one of the three domains of aeRF1 proteins (sequences shorter than 300 amino acids, which included 1,422 sequences), then by removing sequences annotated as a protein fragment (5 sequences), and finally by removing duplicated sequences (104 sequences). This resulted in the dataset of 1,617 sequences of bacterial aeRF1 homologs from 1,353 bacterial species (**Supplementary Data 3**).

To map the identified Balon homologs on the tree of life, we combined the results of the previous searches in the (**Supplementary Data 2**) and (**Supplementary Data 3**) and removed repetitive entries, which resulted in a dataset of 1,898 protein sequences from 1,572 bacterial species (**Supplementary Data 4**). We then aligned the combined sequences using Clustal Omega[76] with default parameters, which resulted in a multiple sequence alignment (Supplementary Data 5) and a phylogenetic tree (**Supplementary Data 6**), which were analysed with JalView[77] and iTol[78], respectively. To compare phylogenetic distribution of Balon, Rmf and RaiA-type hibernation factors, we have repeated homology search using HMMER for Rmf (using the *E. coli* sequence of Rmf as an input) (**Supplementary Data 7**) and RaiA (using the *E. coli* sequences of RaiA as an input) (**Supplementary Data 8**).

Acknowledgements

We thank Zofia Lightowlers, Bert van der Berg and Heath Murray (Newcastle University) for their thoughtful comments on the manuscript, and Dr Johan Turkenburg and Sam Hart for their work supporting the York cryo-EM facility. This work was funded by the Newcastle University NUORS 2021 Award (to K.H-B.), the Medical Research Council (MR/N013840/1 to C.L.E.), a UKRI Future Leader Fellowship (MR/T040742/1 to J.B.), a Wellcome Trust & Royal Society Sir Henry Dale Fellowship (221818/Z/20/Z to C.H.H.), and the Royal Society (RGS/R2/202003 to S.V.M.). This project was undertaken on the NSBL Cluster and the Viking Cluster, which are high-performance compute facility provided by Newcastle University and the University of York, respectively. We are grateful for computational support from the University of York High Performance Computing service, Viking, and the Research Computing team, and support from the Newcastle University Structural Biology Laboratory. We also acknowledge the York cryo-EM facility supported by Wellcome Trust (206161/Z/17/Z) and the York Centre of Excellence in Mass Spectrometry that was created with a capital investment through Science City York and supported by EPSRC (EP/K039660/1; EP/M028127/1) and Yorkshire Forward with funds from the Northern Way Initiative. For the purpose of open access, the authors have applied a CC BY public copyright license to any Author Accepted Manuscript version arising from this submission.

REFERENCES

1 Melnikov, S. *et al.* One core, two shells: bacterial and eukaryotic ribosomes. *Nat Struct Mol Biol* **19**, 560-567, doi:10.1038/nsmb.2313 (2012).
2 Maitra, A. & Dill, K. A. Bacterial growth laws reflect the evolutionary importance of energy efficiency. *Proc Natl Acad Sci U S A* **112**, 406-411, doi:10.1073/pnas.1421138111 (2015).
3 Warner, J. R. The economics of ribosome biosynthesis in yeast. *Trends Biochem Sci* **24**, 437-440, doi:10.1016/s0968-0004(99)01460-7 (1999).
4 Granneman, S. & Tollervey, D. Building ribosomes: even more expensive than expected? *Curr Biol* **17**, R415-417, doi:10.1016/j.cub.2007.04.011 (2007).
5 Usachev, K. S., Yusupov, M. M. & Validov, S. Z. Hibernation as a stage of ribosome functioning. *Biochemistry* **85**, 1434-1442, doi:10.1134/S0006297920110115 (2020).
6 Yoshida, H. & Wada, A. The 100S ribosome: ribosomal hibernation induced by stress. *Wiley Interdiscip Rev RNA* **5**, 723-732, doi:10.1002/wrna.1242 (2014).
7 Basu, A., Shields, K. E., Eickhoff, C. S., Hoft, D. F. & Yap, M. N. Thermal and nutritional regulation of ribosome hibernation in *Staphylococcus aureus*. *J Bacteriol* **200**, doi:10.1128/JB.00426-18 (2018).
8 Li, Y. *et al.* Zinc depletion induces ribosome hibernation in mycobacteria. *Proc Natl Acad Sci USA* **115**, 8191-8196, doi:10.1073/pnas.1804555115 (2018).
9 Trosch, R. & Willmund, F. The conserved theme of ribosome hibernation: from bacteria to chloroplasts of plants. *Biol Chem* **400**, 879-893, doi:10.1515/hsz-2018-0436 (2019).
10 Wang, T. *et al.* Ribosome hibernation as a stress response of bacteria. *Protein Pept Lett* **27**, 1082-1091, doi:10.2174/0929866527666200610142118 (2020).
11 Prossliner, T., Gerdes, K., Sorensen, M. A. & Winther, K. S. Hibernation factors directly block ribonucleases from entering the ribosome in response to starvation. *Nucleic Acids Res* **49**, 2226-2239, doi:10.1093/nar/gkab017 (2021).
12 Sebastian, H. & Finkel, S. E. Absence of ribosome modulation factor alters growth and competitive fitness of *Escherichia coli*. *Microbiol Spectr* **10**, e0223921, doi:10.1128/spectrum.02239-21 (2022).
13 Liponska, A. & Yap, M. F. Hibernation-promoting factor sequesters *Staphylococcus aureus* ribosomes to antagonize RNase R-mediated nucleolytic degradation. *mBio* **12**, e0033421, doi:10.1128/mBio.00334-21 (2021).
14 Li, Y. *et al.* Ribosome hibernation: a new molecular framework for targeting nonreplicating persisters of mycobacteria. *Microbiology* **167**, doi:10.1099/mic.0.001035 (2021).
15 McKay, S. L. & Portnoy, D. A. Ribosome hibernation facilitates tolerance of stationary-phase bacteria to aminoglycosides. *Antimicrob Agents Chemother* **59**, 6992-6999, doi:10.1128/AAC.01532-15 (2015).
16 Akiyama, T. *et al.* Resuscitation of Pseudomonas aeruginosa from dormancy requires hibernation promoting factor (PA4463) for ribosome preservation. *Proc Natl Acad Sci USA* **114**, 3204-3209, doi:10.1073/pnas.1700695114 (2017).
17 van den Elzen, A. M., Schuller, A., Green, R. & Seraphin, B. Dom34-Hbs1 mediated dissociation of inactive 80S ribosomes promotes restart of translation after stress. *EMBO J* **33**, 265-276, doi:10.1002/embj.201386123 (2014).
18 Ben-Shem, A. *et al.* The structure of the eukaryotic ribosome at 3.0 A resolution. *Science* **334**, 1524-1529, doi:10.1126/science.1212642 (2011).
19 Anger, A. M. *et al.* Structures of the human and Drosophila 80S ribosome. *Nature* **497**, 80-85, doi:10.1038/nature12104 (2013).
20 Brown, A., Baird, M. R., Yip, M. C., Murray, J. & Shao, S. Structures of translationally inactive mammalian ribosomes. *Elife* **7**, doi:10.7554/eLife.40486 (2018).
21 Wang, Y. J. *et al.* Lso2 is a conserved ribosome-bound protein required for translational recovery in yeast. *PLoS Biol* **16**, e2005903, doi:10.1371/journal.pbio.2005903 (2018).
22 Wells, J. N. *et al.* Structure and function of yeast Lso2 and human CCDC124 bound to hibernating ribosomes. *PLoS Biol* **18**, e3000780, doi:10.1371/journal.pbio.3000780 (2020).
23 Ehrenbolger, K. *et al.* Differences in structure and hibernation mechanism highlight diversification of the microsporidian ribosome. *PLoS Biol* **18**, e3000958, doi:10.1371/journal.pbio.3000958 (2020).
24 Nicholson, D. *et al.* Adaptation to genome decay in the structure of the smallest eukaryotic ribosome. *Nat Commun* **13**, 591, doi:10.1038/s41467-022-28281-0 (2022).
25 Barandun, J., Hunziker, M., Vossbrinck, C. R. & Klinge, S. Evolutionary compaction and adaptation visualized by the structure of the dormant microsporidian ribosome. *Nat Microbiol* **4**, 1798-1804, doi:10.1038/s41564-019-0514-6 (2019).
26 Polikanov, Y. S., Blaha, G. M. & Steitz, T. A. How hibernation factors RMF, HPF, and YfiA turn off protein synthesis. *Science* **336**, 915-918, doi:10.1126/science.1218538 (2012).
27 Beckert, B. *et al.* Structure of a hibernating 100S ribosome reveals an inactive conformation of the ribosomal protein S1. *Nat Microbiol* **3**, 1115-1121, doi:10.1038/s41564-018-0237-0 (2018).
28 Galmozzi, C. V., Florencio, F. J. & Muro-Pastor, M. I. The cyanobacterial ribosomal-associated protein LrtA is involved in post-stress survival in *Synechocystis sp*. PCC 6803. *PLoS One* **11**, e0159346, doi:10.1371/journal.pone.0159346 (2016).
29 Koonin, E. V. & Aravind, L. Genomics: re-evaluation of translation machinery evolution. *Curr Biol* **8**, R266-269, doi:10.1016/s0960-9822(98)70169-1 (1998).
30 Verma, R. *et al.* Vms1 and ANKZF1 peptidyl-tRNA hydrolases release nascent chains from stalled ribosomes. *Nature* **557**, 446-451, doi:10.1038/s41586-018-0022-5 (2018).
31 Burroughs, A. M. & Aravind, L. The origin and evolution of release factors: implications for translation termination, ribosome rescue, and quality control rathways. *Int J Mol Sci* **20**, doi:10.3390/ijms20081981 (2019).
32 Bowman, J. P., Cavanagh, J., Austin, J. J. & Sanderson, K. Novel Psychrobacter species from Antarctic ornithogenic soils. *Int J Syst Bacteriol* **46**, 841-848, doi:10.1099/00207713-46-4-841 (1996).
33 Gill, C. O. & Newton, K. G. The development of aerobic spoilage flora on meat stored at chill temperatures. *J Appl Bacteriol* **43**, 189-195, doi:10.1111/j.1365-2672.1977.tb00742.x (1977).
34 Mc, L. R., Sulzbacher, W. L. & Mudd, S. *Micrococcus cryophilus*, spec. nov.; a large coccus especially suitable for cytologic study. *J Bacteriol* **62**, 723-728, doi:10.1128/jb.62.6.723-728.1951 (1951).
35 Welter, D. K. *et al.* Free-living, psychrotrophic bacteria of the genus *Psychrobacter* are descendants of pathobionts. *mSystems* **6**, doi:10.1128/mSystems.00258-21 (2021).
36 Farewell, A. & Neidhardt, F. C. Effect of temperature on in vivo protein synthetic capacity in Escherichia coli. *J Bacteriol* **180**, 4704-4710, doi:10.1128/JB.180.17.4704-4710.1998 (1998).
37 Zhang, Y. *et al.* A stress response that monitors and regulates mRNA structure Is central to cold shock adaptation. *Mol Cell* **70**, 274-286 e277, doi:10.1016/j.molcel.2018.02.035 (2018).
38 Gottesman, S. Chilled in translation: adapting to bacterial climate change. *Mol Cell* **70**, 193-194, doi:10.1016/j.molcel.2018.04.003 (2018).
39 Buskirk, A. R. & Green, R. Ribosome pausing, arrest and rescue in bacteria and eukaryotes. *Philos Trans R Soc Lond B Biol Sci* **372**, doi:10.1098/rstb.2016.0183 (2017).
40 Hellen, C. U. T. Translation termination and ribosome recycling in eukaryotes. *Cold Spring Harb Perspect Biol* **10**, doi:10.1101/cshperspect.a032656 (2018).
41 Saito, K. *et al.* Omnipotent role of archaeal elongation factor 1 alpha (EF1alpha in translational elongation and termination, and quality control of protein synthesis. *Proc Natl Acad Sci U S A* **107**, 19242-19247, doi:10.1073/pnas.1009599107 (2010).

42 Stanley, R. E., Blaha, G., Grodzicki, R. L., Strickler, M. D. & Steitz, T. A. The structures of the anti-tuberculosis antibiotics viomycin and capreomycin bound to the 70S ribosome. *Nat Struct Mol Biol* **17**, 289-293, doi:10.1038/nsmb.1755 (2010).
43 Ippolito, J. A. *et al.* Crystal structure of the oxazolidinone antibiotic linezolid bound to the 50S ribosomal subunit. *J Med Chem* **51**, 3353-3356, doi:10.1021/jm800379d (2008).
44 Bulkley, D., Johnson, F. & Steitz, T. A. The antibiotic thermorubin inhibits protein synthesis by binding to inter-subunit bridge B2a of the ribosome. *J Mol Biol* **416**, 571-578, doi:10.1016/j.jmb.2011.12.055 (2012).
45 Hansen, J. L., Moore, P. B. & Steitz, T. A. Structures of five antibiotics bound at the peptidyl transferase center of the large ribosomal subunit. *J Mol Biol* **330**, 1061-1075, doi:10.1016/s0022-2836(03)00668-5 (2003).
46 Song, H. *et al.* The crystal structure of human eukaryotic release factor eRF1: mechanism of stop codon recognition and peptidyl-tRNA hydrolysis. *Cell* **100**, 311-321, doi:10.1016/s0092-8674(00)80667-4 (2000).
47 Brown, A., Shao, S., Murray, J., Hegde, R. S. & Ramakrishnan, V. Structural basis for stop codon recognition in eukaryotes. *Nature* **524**, 493-496, doi:10.1038/nature14896 (2015).
48 Becker, T. *et al.* Structural basis of highly conserved ribosome recycling in eukaryotes and archaea. *Nature* **482**, 501-506, doi:10.1038/nature10829 (2012).
49 Kobayashi, K. *et al.* Structural basis for mRNA surveillance by archaeal Pelota and GTP-bound EF1alpha complex. *Proc Natl Acad Sci U S A* **107**, 17575-17579, doi:10.1073/pnas.1009598107 (2010).
50 Hilal, T. *et al.* Structural insights into ribosomal rescue by Dom34 and Hbs1 at near-atomic resolution. *Nat Commun* **7**, 13521, doi:10.1038/ncomms13521 (2016).
51 Frolova, L. Y. *et al.* Mutations in the highly conserved GGQ motif of class 1 polypeptide release factors abolish ability of human eRF1 to trigger peptidyl-tRNA hydrolysis. *RNA* **5**, 1014-1020, doi:10.1017/s135583829999043x (1999).
52 Polikanov, Y. S., Steitz, T. A. & Innis, C. A. A proton wire to couple aminoacyl-tRNA accommodation and peptide-bond formation on the ribosome. *Nat Struct Mol Biol* **21**, 787-793, doi:10.1038/nsmb.2871 (2014).
53 Maguire, B. A., Beniaminov, A. D., Ramu, H., Mankin, A. S. & Zimmermann, R. A. A protein component at the heart of an RNA machine: the importance of protein l27 for the function of the bacterial ribosome. *Mol Cell* **20**, 427-435, doi:10.1016/j.molcel.2005.09.009 (2005).
54 Aravind, L. & Koonin, E. V. Eukaryote-specific domains in translation initiation factors: implications for translation regulation and evolution of the translation system. *Genome Res* **10**, 1172-1184, doi:10.1101/gr.10.8.1172 (2000).
55 Burroughs, A. M. & Aravind, L. The origin and evolution of release factors: implications for translation termination, ribosome rescue, and quality control pathways. *Int J Mol Sci* **20**, doi:10.3390/ijms20081981 (2019).
56 Park, H. D. *et al.* Rv3133c/dosR is a transcription factor that mediates the hypoxic response of *Mycobacterium tuberculosis*. *Mol Microbiol* **48**, 833-843, doi:10.1046/j.1365-2958.2003.03474.x (2003).
57 Liu, D. *et al.* Rv2629 overexpression delays *Mycobacterium smegmatis* and *Mycobacteria tuberculosis* entry into log-phase and increases pathogenicity of *Mycobacterium smegmatis* in mice. *Front Microbiol* **8**, 2231, doi:10.3389/fmicb.2017.02231 (2017).
58 Avican, K. *et al.* RNA atlas of human bacterial pathogens uncovers stress dynamics linked to infection. *Nat Commun* **12**, 3282, doi:10.1038/s41467-021-23588-w (2021).
59 Manwar, M. R. *et al.* The bacterial RNA ligase RtcB accelerates the repair process of fragmented rRNA upon releasing the antibiotic stress. *Sci China Life Sci* **63**, 251-258, doi:10.1007/s11427-018-9405-y (2020).
60 Filipowicz, W. Making ends meet: a role of RNA ligase RtcB in unfolded protein response. *EMBO J* **33**, 2887-2889, doi:10.15252/embj.201490425 (2014).
61 Temmel, H. *et al.* The RNA ligase RtcB reverses MazF-induced ribosome heterogeneity in Escherichia coli. *Nucleic Acids Res* **45**, 4708-4721, doi:10.1093/nar/gkw1018 (2017).
62 Tian, Y. *et al.* Sequential rescue and repair of stalled and damaged ribosome by bacterial PrfH and RtcB. *Proc Natl Acad Sci U S A* **119**, e2202464119, doi:10.1073/pnas.2202464119 (2022).
63 Huang, H. Y. & Hopper, A. K. Multiple layers of stress-induced regulation in tRNA biology. *Life (Basel)* **6**, doi:10.3390/life6020016 (2016).
64 Apweiler, R. *et al.* UniProt: the universal protein knowledgebase. *Nucleic Acids Res* **32**, D115-119, doi:10.1093/nar/gkh131 (2004).
65 Ishihama, Y. *et al.* Exponentially modified protein abundance index (emPAI) for estimation of absolute protein amount in proteomics by the number of sequenced peptides per protein. *Mol Cell Proteomics* **4**, 1265-1272, doi:10.1074/mcp.M500061-MCP200 (2005).
66 Punjani, A., Rubinstein, J. L., Fleet, D. J. & Brubaker, M. A. cryoSPARC: algorithms for rapid unsupervised cryo-EM structure determination. *Nat Methods* **14**, 290-296, doi:10.1038/nmeth.4169 (2017).
67 Scheres, S. H. RELION: implementation of a Bayesian approach to cryo-EM structure determination. *J Struct Biol* **180**, 519-530, doi:10.1016/j.jsb.2012.09.006 (2012).
68 Casanal, A., Lohkamp, B. & Emsley, P. Current developments in Coot for macromolecular model building of electron cryo-microscopy and crystallographic data. *Protein Sci* **29**, 1069-1078, doi:10.1002/pro.3791 (2020).
69 David, A., Islam, S., Tankhilevich, E. & Sternberg, M. J. E. The AlphaFold database of protein structures: a biologist's guide. *J Mol Biol* **434**, 167336, doi:10.1016/j.jmb.2021.167336 (2022).
70 Polikanov, Y. S., Melnikov, S. V., Soll, D. & Steitz, T. A. Structural insights into the role of rRNA modifications in protein synthesis and ribosome assembly. *Nat Struct Mol Biol* **22**, 342-344, doi:10.1038/nsmb.2992 (2015).
71 Pettersen, E. F. *et al.* UCSF ChimeraX: Structure visualization for researchers, educators, and developers. *Protein Sci* **30**, 70-82, doi:10.1002/pro.3943 (2021).
72 Adams, P. D. *et al.* The Phenix software for automated determination of macromolecular structures. *Methods* **55**, 94-106, doi:10.1016/j.ymeth.2011.07.005 (2011).
73 Madej, T. *et al.* MMDB and VAST+: tracking structural similarities between macromolecular complexes. *Nucleic Acids Res* **42**, D297-303, doi:10.1093/nar/gkt1208 (2014).
74 Prakash, A., Jeffryes, M., Bateman, A. & Finn, R. D. The HMMER web server for protein sequence similarity search. *Curr Protoc Bioinformatics* **60**, 3 15 11-13 15 23, doi:10.1002/cpbi.40 (2017).
75 Davis, I. W. *et al.* MolProbity: all-atom contacts and structure validation for proteins and nucleic acids. *Nucleic Acids Res* **35**, W375-383, doi:10.1093/nar/gkm216 (2007).
76 Sievers, F. & Higgins, D. G. Clustal Omega for making accurate alignments of many protein sequences. *Protein Sci* **27**, 135-145, doi:10.1002/pro.3290 (2018).
77 Waterhouse, A. M., Procter, J. B., Martin, D. M., Clamp, M. & Barton, G. J. Jalview Version 2: a multiple sequence alignment editor and analysis workbench. *Bioinformatics* **25**, 1189-1191, doi:10.1093/bioinformatics/btp033 (2009).
78 Letunic, I. & Bork, P. Interactive tree of life (iTOL): an online tool for phylogenetic tree display and annotation. *Bioinformatics* **23**, 127-128, doi:10.1093/bioinformatics/btl529 (2007).